Research Article

Study Behavior of Hollow Reinforced Concrete Beams

Nasr Z. Hassan, Hala M. Ismael and Amany M. Salman[*]

Civil Engineering Department, Helwan University, Cairo, Egypt

Abstract

The concept of opening or hollow in the structure elements is made to meet the architectural demands through passing mechanical or electrical runs, in addition creating reduction in weight and savings in materials. This concept done by installing circular PVC pipe in tension zone of reinforced concrete beams as concrete below the neutral axis acts as a stress transfer medium between compression and tension zone. A total of 10 reinforced concrete beams of size 2500mm x 200mm x 300mm were casted and tested by four point bending test. The results such as crack load, ultimate load, crack pattern, failure modes, loads deflection curves, stiffness, ductility index and absorbed energy for all tested beams were studied. The test results indicated that, the pipe diameter less than 0.25 width of under or over reinforced beams their center at two investigated location (0.53*d) and (0.60*d) had no effect on the capacity and stiffness of beam. For larger pipe diameter, the ultimate capacity of beams depend on its location and flexural and shear reinforcement ratio, crack width of beams with inserted PVC pipe were wider and failure modes were brittle diagonal shear failure. Analytical study is carried out using ANSYS 14.5 program and the maximum difference in predicting failure load is about 19.00% so the use of computer software to model these beams is much faster and saving cost.

Keywords: Hollow beams, PVC pipe, Neutral axis, Experimental program, Finite Element Analysis (FEA), ANSYS

1. Introduction

The opening or hollow in the structure elements are becoming popular in nowadays building design and have been increasingly applied in the construction of buildings, bridges, offshore structures, and towers for satisfaction requirements of passing mechanical and electrical runs due to the aesthetic appeal and other benefits as creating reduction in weight and savings in materials.

In this paper an experimental and analytical study on hollow beam is done by inserting PVC pipe in tension zone at various depths and with different size. As concrete below the neutral axis acts as a stress transfer medium between the compression and tension zone.

The reduction of surface area of the beam due to adding PVC pipe will influence on its performance and behavior in bending moment and shear resistance therefore, the experimental test and analytical study are done to identify the flexural strength, shear strength, deflection profile and crack pattern of the hollow beams and provide better recommendation and suggestion about optimum depth and size for hollow section beams.

According to (ECP 203, 2017) in design doubly reinforced concrete beams the contribution of tensile stress of concrete is neglected because it has cracked and therefore cannot hold any tension. In this type of beam, the internal couple is balanced between the tension steel and the combination of the concrete compression block and compression steel. The neutral axis is where zero stress in the member, the distance from the compression face to the neutral axis is denoted as (C) as shown in Figure (1).
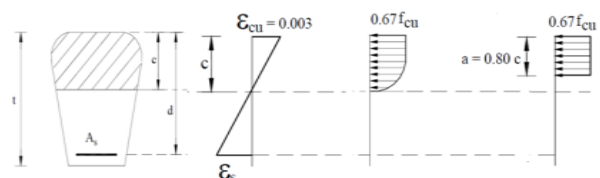

Fig. 1 Stress-Strain Distribution in Simple Reinforced concrete Beam

The depth of neutral axis is calculated by considering M30 grade concrete and 400MPa yield tensile strength of steel with an effective cover of 25mm. according to (ECP 203, 2017) ((C_{max} = 0.40*d) and (μ_{max} = 0.013)) And here two sections were designed**.** The depth of neutral axis for under reinforced section (μ = 0.010) calculated as follow:

$$T = Cc + Cs$$

$$As * Fy = 0.67 * Fcu * b * a + As` * Fy \tag{1}$$

$$a = 44.00mm \rightarrow C = 1.25 * a = 55.00mm \tag{2}$$

$C < Cmax$, So it is under reinforced section.

The depth of neutral axis for over reinforced section ($\mu = 0.018$) calculated as follow:

$$As * Fs = 0.67 * Fcu * b * a + As` * Fy \tag{3}$$

$$\frac{1.25*a}{d} = \frac{600}{600+Fs} \tag{4}$$

From equation (3) and equation (4):
a = 117mm → Fs = 524MPa → Fs > Fy
$C = 1.25 * a = 146mm \rightarrow C > Cmax$
So it is over reinforced section.

2. Objective of the Work

The main objective of this paper is studying effect of the following parameters on behavior of hollow section beams to get optimum depth and size:

1) Tension reinforcement ratio (0.010 and 0.018)
2) Diameter of PVC pipe (50mm and 75mm)
3) Center position of PVC pipe from the top of section (160mm and 180mm)
4) Simulate and analyze behavior of all tested beams by using ANSYS 14.5 finite element program to provide a reliable method for predicting the behavior of experimental results

3. Related Work

• (Alnuaimi *et al*, 2008) compared between solid and hollow reinforced concrete beams. (Solid and hollow beam with the same reinforcement) shows that all solid beams cracked at higher loads than the hollow beams. The hollow beams failed close to the design loads while the solid beams failed in the higher load. This indicates that the core contributes to the ultimate load resistance of the section and cannot be ignored in term of combined load of bending, shear and torsion.

• (Jain Joy and Rajesh Rajeev, 2014) attempted to reduce weight and cost of the reinforced concrete structures by replacing the concrete in and near the neutral axis. By placing a PVC pipe instead, nine specimens were cast and tested; three beams as reference, three made hollow in their neutral axis using 40mm diameter PVC pipe and the remaining three made hollow in their neutral axis using 50mm diameter PVC pipe. They found that there is not much difference in the load carrying capacity of solid control beam section and that of beam section with hollow neutral axis. However the hollow section decrease in load capacity and increase in corresponding deflection also the volume of concrete decreases, the material cost reduces which decreases the construction cost.

• (Thaar S. Salaman, 2015) studied the effect of installation of PVC pipe on behavior of reinforced concrete moderate deep beams. The test results indicated that the pipe diameter less than 1/3 of the beam width had limited effect on the capacity and rigidity of beam. For larger pipes, the ultimate strength of beams decreased between 16.7% and 33.3% and the beams stiffness decreased between 103% and 297%.

• (S.Manikandan, S.Dharmar and S.Robertravi, 2016) created experimental study on flexural behavior of reinforced concrete hollow core sandwich beams with and without hollow core in circular 75mm diameter and square 70mm used tension zone. They found that the flexural strength and yield deformation of RC beam with square hollow is less compared with RC solid and RC circular hollow beam.

• (Dhinesh.N.P and Satheesh.V.S, 2017). Presented a detailed study about flexural behavior on hollow reinforced square beam, all beams tested by three points loading. It was found that the ultimate load carrying capacity of the beam is high in tensile zone of hollow core when compared to other zones of hollow core.

4. Material and Experimental Program

4.1 Materials

All materials used in this experimental work are local materials and match with (ECP 203, 2017) limits (sand, gravel, ordinary Portland cement and drinking water).
All batches used were of good quality, clean and free from organic material as shown in Figure 2. Concrete used had a compressive strength about 30MPa after 28 days and 3.32MPa split tensile strength. Two diameters (50mm and 75mm) of PVC have been used only as a filler material. The mix design of used concrete had the following composition per 1-meter cube in Table1. The main longitudinal reinforcement had yield stress of 400MPa, and the yield stress of the stirrups is 240MPa.

Fig. 2 Cement, Gravel, Sand and PVC Pipe Used

Table 1 Mix Design for M30 Grade Concrete

Portland cement Kg/m³	350
sand Kg/m³	800
gravel Kg/m³	1200
water Kg/m³	175
water cement ratio	0.50
Mix Ratio	1 : 2.28 : 3.42 : 0.50

4.2 Experimental Program

A total of ten specimens were casted and tested, 2 solid beams as control beam and other hollow beams in four groups each group has two beams. The tested parameters are clarified in Table 2. And all tested beams have the same dimensions (2500mm x200mm x300mm) and the same top reinforcement 2Ø10. as shown in Figure 3

Table 2 Detailed Parameters of Tested beams

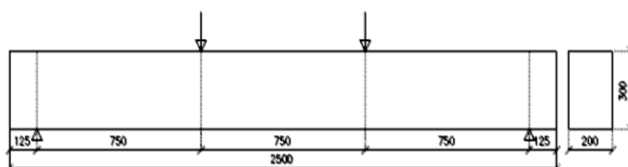| Group	Beam	PVC Diameter	PVC position	A_s	Stirrup/L
G.0	B-0-1	-----	-----	3Ø16	6Ø8
	B-0-2			5Ø16	10Ø8
G.1	B-1-1	50mm	160mm	3Ø16	6Ø8
	B-1-3			5Ø16	10Ø8
G.2	B-2-1	50mm	180mm	3Ø16	6Ø8
	B-2-3			5Ø16	10Ø8
G.3	B-3-1	75mm	160mm	3Ø16	6Ø8
	B-3-3			5Ø16	10Ø8
G.4	B-4-1	75mm	180mm	3Ø16	6Ø8
	B-4-3			5Ø16	10Ø8

Fig. 3 Concrete Dimension

Figure 4 shows the preparation of the reinforcement cages of the beams and hanging PVC pipes according their center location.

To measure the strain in tension bars and stirrups, electrical strain gauges with length 10mm were attached to the main reinforcing bars at flexural zone and 6mm were attached to stirrups at shear zone. The steel strain was measured and recorded using digital strain indicator connected to data acquisition system. Figure 5 shows the fixing of the strain gauges and measuring its efficiency.

The reinforcing cages were placed in the wooden forms which coated with oil. Then Concrete was prepared in a tilting rotary drum mixer and casted in the form. Electrical vibrator was used to compact

concrete mechanically, Figure 6 shows mixing, casting and compacting of concrete. After three days the wooden forms were removed. Specimens were cured for 28 days by covering surface by water and sheets.

Fig. 4 Reinforcing Cages and Holding PVC Pipes

Fig. 5 Fixing Strain gauge and measuring its Efficiency

Fig. 6 Mixing, Casting and Compacting Concrete

4.3 Test Setup and Procedure

The specimens are mounted on beam testing frame of 50 ton capacity. The beams were tested as a two point loading system using a hydraulic jack attached to the loading frame. Three dial gauges were used to measure vertical deflection of the beams. The first one was located at the middle of the span and others under two points of loading. At the time of testing, the specimen was painted with white cement to help the visual crack

detection during testing process. The load was applied gradually with constant rate and the readings of measurements devices were recorded in paper sheet at every increment of load. The cracking load was recorded once the first crack noticed. The specimen was loaded until reaching failure load. A data logger and a reader were used to measure strains in bars and loading values as shown in Figure 7.

Fig. 7 Beam Test Setup, Dial Gauge and Load Cell

5. Experimental Results

5.1 Cracking Load and Ultimate Load

For each beam Table 2 summarizes the tested result of the experimental program includes the first cracking load and its deflection (P_{cr} and Δ_{cr}) and maximum load and its deflection (P_{max} and Δ_{max}).

Table 3 Cracking Load and Ultimate Load

Group	Beam	P_{cr} (kN)	Δ_{cr} (mm)	P_{max} (kN)	Δ_{max} (mm)
G.0	B-0-1	55.70	1.97	208.10	14.81
	B-0-2	114.50	4.15	249.00	15.32
G.1	B-1-1	71.70	2.82	214.10	13.33
	B-1-3	84.60	2.56	260.0	11.53
G.2	B-2-1	68.70	2.43	209.10	9.78
	B-2-3	78.60	2.40	277.8	17.02
G.3	B-3-1	45.80	1.65	224.10	16.98
	B-3-3	72.70	2.19	273.00	11.84
G.4	B-4-1	46.80	1.76	185.20	12.79
	B-4-3	67.70	2.15	257.90	11.09

By comparing results of beams with under reinforced section as shown in Figure.8 there is no variation in the load carrying capacity of the control beams and others with PVC pipes except that B-4-1 which has the larger PVC diameter and lower position in tension zone. For beams with over reinforced section the load carrying capacity not affected at all as shown in Figure 9.
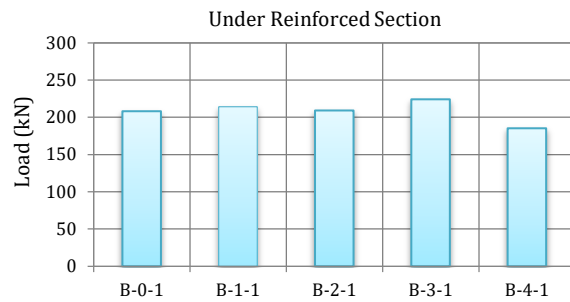
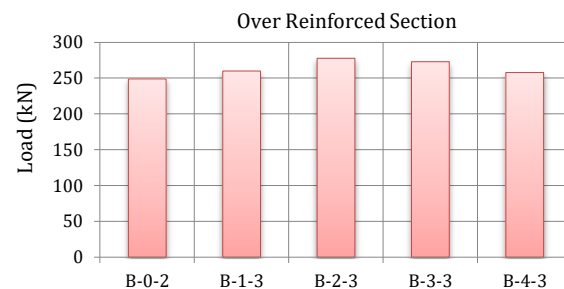**Fig.8** Ultimate Load for Beams with Under Reinforced Section

Fig.9 Ultimate Load for Beams with Over Reinforced Section

5.2 Load Deflection Curves

The load deflection curves of tested beams with under reinforced sections and over reinforced sections for point at the mid span are shown in Figure 10 and Figure 11 respectively.
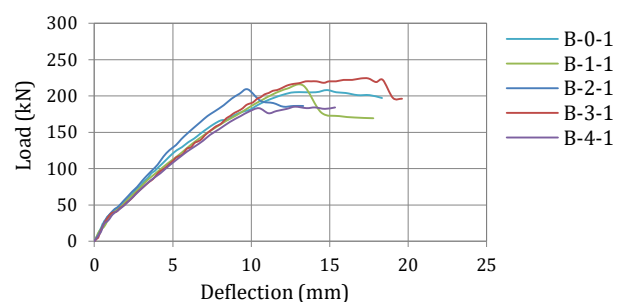
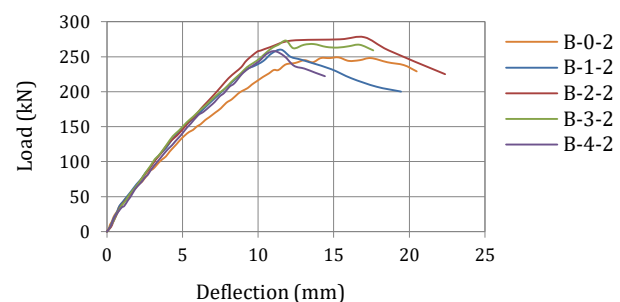**Fig. 10** Load-Deflection Curves for Beams with under Reinforced Section

Fig. 11 Load-Deflection Curves for Beams with Over Reinforced Section

The figures clearly show that all specimens behave the same manner as all beams Load-Deflection Curves remained elastic till the occurrence of first crack then due to further increase in the load the deflection values will increase but the load values will not be in proportion to deflection and material loses elasticity undergoing plastic deformation and the steel reinforcement yields. Then the rate of the deflection increased up to complete failure. The curve of beams with PVC pipe became steep after ultimate load.

5.3 Cracks Development and Failure Mode

Fig.12 Crack Pattern for Beams with Under Reinforced Section

Figure 12 and Figure 13 show cracks development for all tested beams. For all beams the initial cracks started at middle section of the beam when the applied load reached to the rupture strength of the concrete then shear cracks developed from the supporting points and widened up as the load increased within shear span between the applied load and the support. As loading increased, more flexural and diagonal cracks were formed and cracks became wider and increased in length. Shear cracks passed toward the compression zone and continued to the loading point. The width of the inclined shear cracks near the supports increased faster causing shear failure. For beams with PVC pipe the crack widths of beams were wider and the main shear crack not reached to supports as solid beam.

Fig.13 Crack Pattern for Beams with Over Reinforced Section

5.4 Strains in Tension Reinforcement and Stirrup

Electrical strain gauge with length 10 mm was attached to the main reinforcing bar at flexural zone (mid span) and with length 6 mm was attached to stirrups at shear zone (located at 150 mm from left support) to measure the strain in tension bar and stirrups. Since the yield strain and ultimate strain of used tension steel bars were calculated from equations (5) and (6) respectively:

$$\varepsilon y = \frac{Fy}{Es} = \frac{400}{200000} = 0.002 \tag{5}$$

$$\varepsilon u = \frac{Fu}{Es} = \frac{600}{200000} = 0.003 \tag{6}$$

And the yield strain and ultimate strain of used stirrups were calculated from equations (7) and (8) respectively:

$$\varepsilon y = \frac{Fy}{Es} = \frac{240}{200000} = 0.0012 \tag{7}$$

$$\varepsilon u = \frac{Fu}{Es} = \frac{350}{200000} = 0.0018 \tag{8}$$

Table 4 illustrates values of maximum strain in tension bars and stirrups (ε_1 and ε_2 respectively) and failure mode with respect to strain values for all tested beams. For beam B-0-1 the maximum strain of tension bar at failure is 0.003 and maximum strain of stirrup is 0.0016 which are in a reasonable agreement with the values of corresponding yielding.

Table 4 Maximum Values of Strain in Tension Bars and Stirrups with Failure Type for Each Beam

Group	Beam	$\varepsilon_1/10^6$	$\varepsilon_2/10^6$	Failure type
G.0	B-0-1	3051	1655	Flexural
	B-0-2	2634	2596	Shear
G.1	B-1-1	2941	-----	Shear
	B-1-3	2326	-----	Shear
G.2	B-2-1	2495	834	Shear
	B-2-3	1793	1376	Shear
G.3	B-3-1	3376	1200	Flexural
	B-3-3	2413	903	Shear
G.4	B-4-1	2382	1693	Shear
	B-4-3	2538	1137	Shear

The relation between the strain of tension bar and the applied load for beams with under reinforced section and beams with over reinfor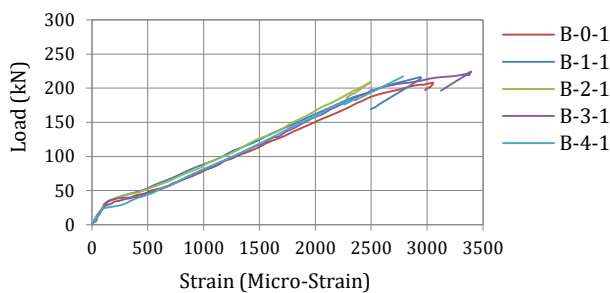ced section are shown in Figure14 and Figure15 respectively. And the relation between the strain of stirrups and the applied load for beams with under reinforced section and beams with over reinforced section are shown in Figure.16 and Figure17 respectively.

Fig.14 Load-Strain Curve of Tension Bar for Beams with under Reinforced Section
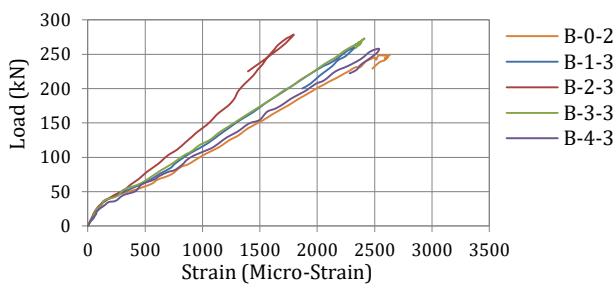

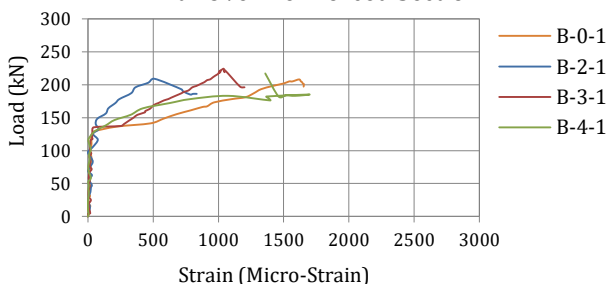**Fig.15** Load-Strain Curve of Tension Bar for Beams with Over Reinforced Section

Fig.16 Load-Strain Curve of Stirrup for Beams with under Reinforced Section
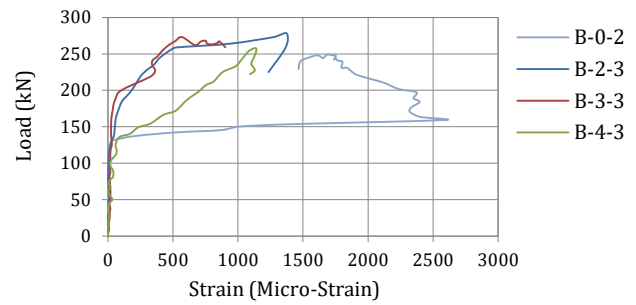

Fig.17 Load-Strain Curve of Stirrup for Beams with Over Reinforced Section

5.5 Stiffness, Ductility Index and Absorbed Energy

Stiffness, ductility index and absorbed energy values for all tested beams are listed in Table 5. Stiffness is calculated as the slope of the first straight part of the load-deflection curve at value cracking load.

Table 5 Stiffness, Ductility Index and Absorbed Energy

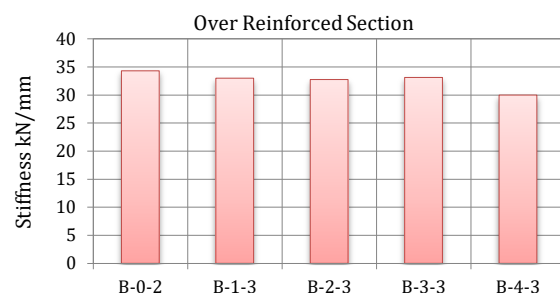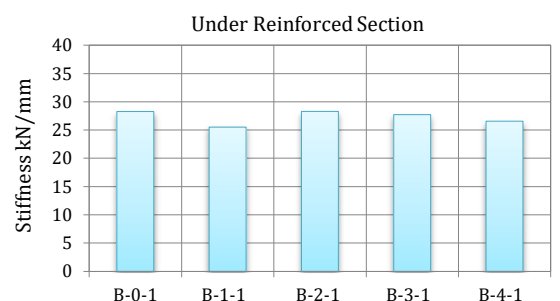| Group	Beam	Stiffness kN/mm	Ductility Index μ_d%	Absorbed Energy kN.mm
G.0	B-0-1	28.27	6.52	2789.99
	B-0-2	34.30	3.94	3778.66
G.1	B-1-1	25.51	5.33	2544.86
	B-1-3	32.99	5.17	3234.07
G.2	B-2-1	28.29	5.79	2135.93
	B-2-3	32.75	5.42	3774.02
G.3	B-3-1	27.72	9.29	3128.47
	B-3-3	33.12	7.05	3412.56
G.4	B-4-1	26.56	7.72	2007.47
	B-4-3	29.98	5.71	2411.39

Fig.18 Stiffness of Beams with under and over Reinforced Sections

Ductility can be defined as the ability of material to undergo large deformations without rupture before failure so ductility index (μ_d) is calculated as the percentage of increase in elongation (from cracking stage to failure stage) relative to elongation at cracking stage:

$$\mu_d = \frac{\delta_{ul} - \delta_{cr}}{\delta_{cr}} \tag{9}$$

Where: δ_{ul} is mid span deflection at ultimate load and δ_{cr} is mid span deflection at cracking load. The energy absorption based on displacement is Ability of material to absorb energy prior to failure and calculated as the area under the load-deflection curve till failure load.
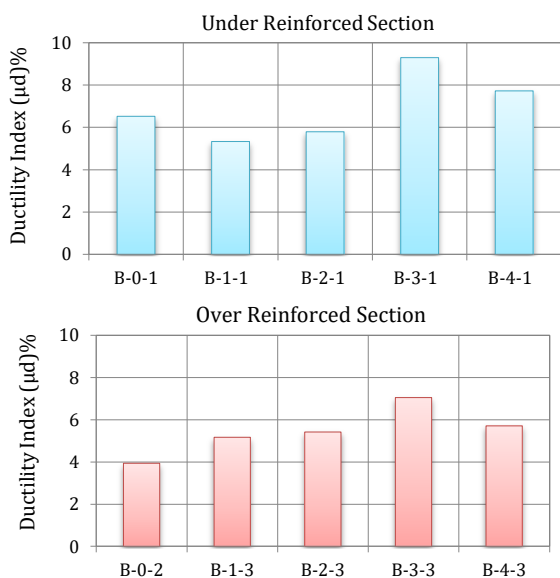

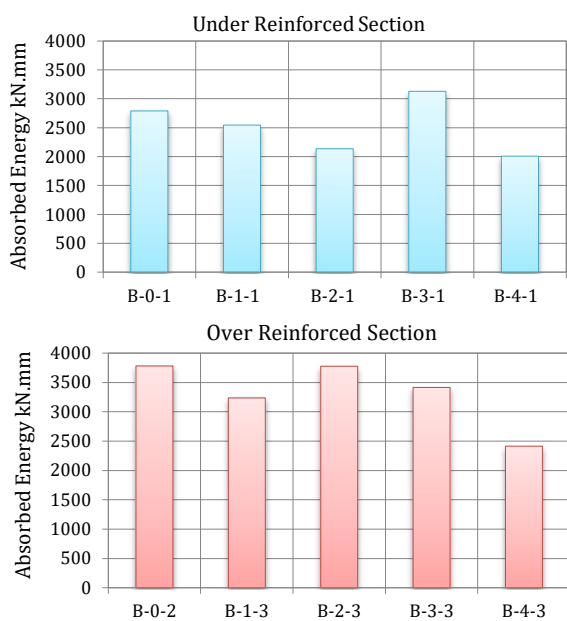**Fig.19** Ductility Index of Beams with under and over Reinforced Sections

Fig.20 Absorbed Energy of Beams with under and over Reinforced Sections

6. Analytical Study

The use of computer software to analyze concrete structural components is become now one of much faster and extremely cost-effective methods. ANSYS 14.5 finite element program is used in this paper to simulate and analyze behavior of tested beams and compare between experimental and analytical results. Three stages are required for modeling and analysis element with ANSYS:

- Pre-processing includes define the element type, Real constants, Material properties, Sections, Create the model and mapped mesh.
- Analysis solver by applying the boundary conditions, Loads and Solution.
- Post-processing of results like loads increment, deflections and stress contours.

6.1 Element Type and Real Constant

Table 6 Element Type Used

Concrete	SOLID65
Steel Reinforcement	LINK180
PVC pipe	SHELL181
Loading & Supporting Steel Plates	SOLID 185

Table 7 Real Constant for Used Element

Real Constant	Element Type	Constant	
1. Concrete	SOLID65	-------	
2. Main Reinforcement	LINK180	Cross-Sectional Area (mm²)	201
		Initial strain (mm/mm)	0.00
3. Secondary Reinforcement	LINK180	Cross-Sectional Area (mm²)	785
		Initial strain (mm/mm)	0.00
4. Stirrups	LINK180	Cross-Sectional Area (mm²)	50.0
		Initial strain (mm/mm)	0.00

6.2 Material Properties and Define Section

Proper material models are needed to obtain accurate analysis. SOLID65 element requires linear isotropic and multi-linear isotropic material properties to properly model concrete. Table 7 lists concrete properties. EX is the modulus of elasticity of the concrete and calculated based on the Egyptian Code equation (ECP-203-2017). PRXY is the Poisson's ratio (v), it was assumed to be 0.2 for all specimens.

$$E_c = 4400 * \sqrt{Fcu} \ (MPa) \tag{9}$$

The multi-linear isotropic material uses the Von Mises failure criterion to define the failure of the concrete.

The multi-linear stress-strain curve used to help with convergence of the nonlinear solution algorithm was obtained by the following equations (Desayi, 1964):

$$f = \frac{E_c * \varepsilon}{1 + \left(\frac{\varepsilon}{\varepsilon_o}\right)^2} \qquad (10)$$

$$\varepsilon_o = \frac{2 * fc`}{E_c} \qquad (11)$$

ε_o is strain at the ultimate cylinder compressive strength $f_c`$ and according to the (ECP-203-2017), it can be taken equal to $0.8F_{cu}$. Concrete material model in (ANSYS, SAS 2012) requires some constants be defined as shear transfer coefficient β which represents conditions of the crack face and determines the amount of shear transferred a cross the crack. The value of β ranges from (0.0 to 1.0), Uniaxial tensile cracking stress f_r and Uniaxial crushing stress $f_c`$.

Table 8 Material Properties for Concrete

Linear Isotropic		Multi-Linear Isotropic		Concrete	
EX	24100	strain	Stress	β_o	0.30
PRXY	0.20	0.0003	7.60	β_c	0.90
		0.0006	13.35	f_r	3.32
		0.0009	18.15	$f_c`$	24.0
		0.0015	23.28		
		0.0018	24.00		
		0.002	24.00		
		0.003	24.00		

LINK180 element is used for all steel reinforcement in the beams and it requires linear isotropic and Bilinear Isotropic material properties, SOLID 185 element is used to model the loading and support plates to avoid stress concentration and it requires linear isotropic material properties also SHELL181 element requires linear isotropic material properties as shown in Table 8. Then SHELL181 element needs to define sections by adding shell thickness and material properties used, the thickness of PVC pipes with diameters of 50 mm and 75 mm is 2.2mm and 2.4mm respectively.

Table 9 Material Properties for Steel Reinforcement, Steel Plates and PVC pipe

	Linear Isotropic		Bilinear Isotropic	
2.LINK180	EX	$2*10^5$	Yield Stress	400
	PRXY	0.30	Tang Mod	0.00
	Linear Isotropic		Bilinear Isotropic	
3.LINK180	EX	$2*10^5$	Yield Stress	240
	PRXY	0.30	Tang Mod	0.00
	Linear Isotropic			
4.SOLID 185	EX	$2*10^5$		
	PRXY	0.30		
	Linear Isotropic			
6.SHELL181	EX	3300		
	PRXY	0.40		

6.3 Modeling and Meshing

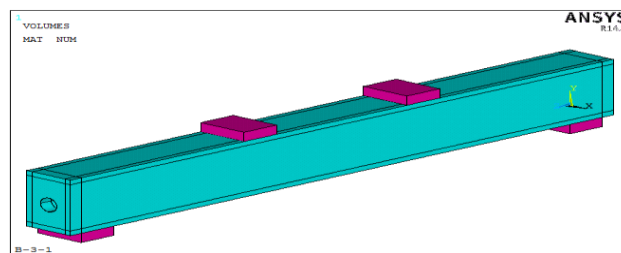The beam, plates, and supports were modeled as volumes as in Figure21.

Fig.21 Volumes Created in ANSYS for Beam Models

The mesh is set up by creating square elements. The volume sweep command was used to mesh the steel plate, support and beam. This properly sets the width and length of elements in the plates to be consistent with the elements and nodes in the concrete portions of the model. The command (merge items) is used to merge separate entities that have the same location. The overall mesh of the concrete, plate, and support volumes is shown in Figure22.
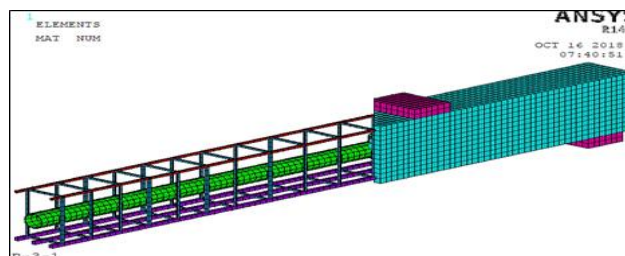

Fig.22 Meshing of Beam Model with PVC Pipe

6.4 Loads and Boundary Conditions

To ensure that the model has the same way as the experimental beam, displacement boundary conditions are needed. For hinged support a single line of nodes on the plate were given constraint in the UY, UX and UZ directions, applied as constant values of (0.0) and for roller support a single line of nodes on the plate were given constraint in the UY, UZ applied as constant values of (0.0). The force (P) is applied across the entire centerline of the plate as shown in Figure23.
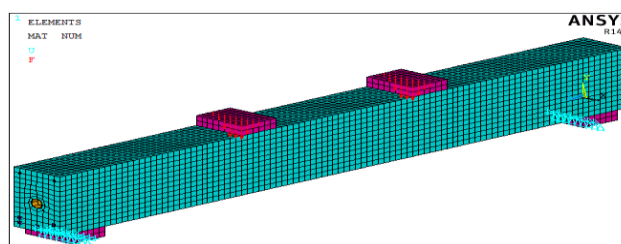

Fig.23 Boundary Conditions for Loading and Supporting Plates

6.5 Non Linear Solution

For these models, the static analysis type is chosen. In nonlinear analysis, the total applied load is divided into a series of load increments called load steps. At the completion of each incremental solution, the stiffness matrix of the model is adjusted to reflect nonlinear changes in structural stiffness before proceeding to the next load increment. The ANSYS program uses Newton-Raphson equilibrium iterations for updating the model stiffness (ANSYS, SAS 2012). The convergence tolerance limits were 0.50% for force checking and 5.00% for displacement checking to obtain convergence of the solutions. The automatic time stepping in the ANSYS program predicts and controls load step sizes for which the maximum and minimum load step sizes are required. Failure for each model was identified when the program gives a message specifying that the model has a significantly large deflection exceeding the displacement limitation of the ANSYS program.
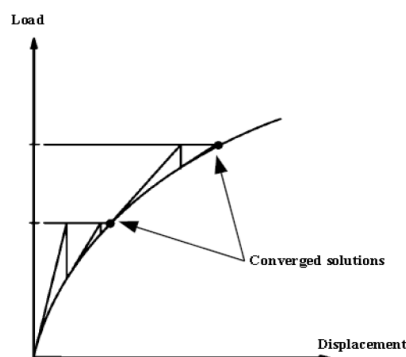
Fig.24 Newton-Raphson Iterative Solution

7. Analytical Study Results

Table 10 shows comparison between experimental and finite element results at failure stage to verify the accuracy of using finite element models.

Table 10 Comparison between Experimental and Analytical Results

Beam. No	$P_{ul.Exp}$ (kN)	$\delta_{ul.Exp}$ (mm)	$P_{ul.FEM}$ (kN)	$\delta_{ul.FEM}$ (mm)	$P_{ul.Exp}/P_{ul.FEM}$
B-0-1	208.10	14.81	188.92	10.23	1.10
B-0-2	249.00	15.32	246.6	8.90	1.01
B-1-1	214.10	13.33	185.84	8.52	1.15
B-1-3	260.00	11.53	250.10	8.80	1.04
B-2-1	209.10	9.87	189.25	10.40	1.10
B-2-3	277.80	17.02	246.20	8.56	1.13
B-3-1	224.10	16.98	187.60	11.08	1.19
B-3-3	273.00	11.84	244.30	8.47	1.12
B-4-1	185.20	12.79	183.50	11.62	1.01
B-4-3	257.90	11.09	242.90	8.75	1.06

From Table 10 we can see that finite element ultimate load results are slightly smaller than experimental ultimate load with maximum difference (19.00%) this is due to:

- Finite element model does not have toughening mechanisms as in experimental beams like the grain bridging process, interlocking between the cracked faces, crack tips blunted by voids, and the crack branching process.
- Idealized stress-strain curve for the steel was perfectly plastic stress-strain curve and also the concrete after the ultimate compressive stress causes the lower failure load in the finite element models.

The deflection contours of the finite element model B-0-2 at the last converged load step is shown in Figure. 25 the contour lines for all models have the same shape but differ in the value.
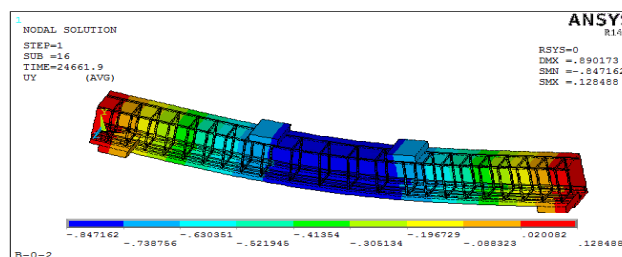
Fig.25 Deflection Contours of Beam Model B-0-2

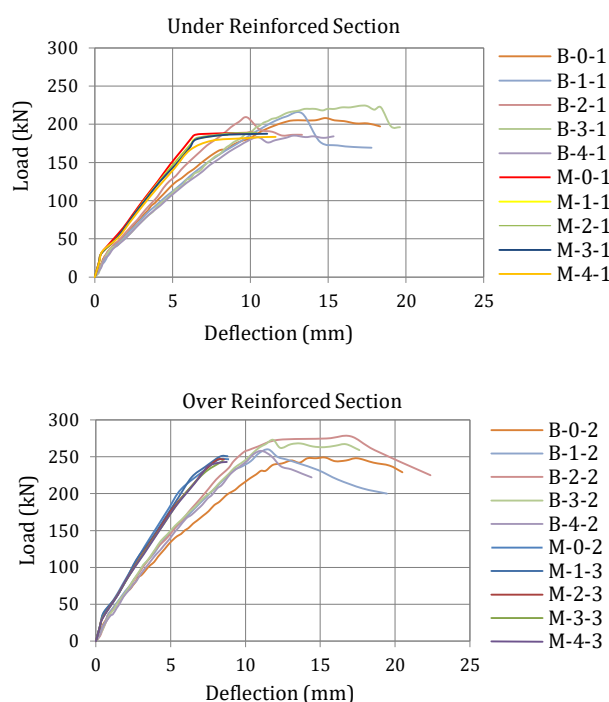### 7.1 Load Deflection Curves

Fig.26 Load Deflection Curves for F.E Models and Tested Beams with Under and Over Reinforced Section

Figure 26 shows the load deflection curves at mid span of finite element models with experimental tested beams for under and over reinforced section. It was found that the curve of finite element model is in close agreement with the experimental curve at the elastic period and when the curve goes to nonlinear Finite element model becomes stiffer than the corresponding experimental curve and this is due to several factors:

- The finite element models do not include the micro-cracks produced by drying shrinkage in the concrete or handling of the beams.
- The bond between the concrete and reinforcing steel is assumed to be perfect (no slip) in the finite element analyses but for the actual beams slip occurs.
- Inability of ANSYS to model the strain softening effect of concrete, the load deflection curve is only available till the ultimate load. Then the program gives a message specifying the model has a significant large deflection exceeds the displacement limitation of ANSYS program. This indicates failure of the beam.

7.2 Cracking Pattern

A cracking sign in ANSYS represented by a circle appears when a principal tensile stress exceeds the ultimate tensile strength of the concrete. And it appears perpendicular to the direction of the principal stress and crushing is shown with an octahedron outline. The first crack at integration point is shown with a red circle outline, the second crack with a green outline, the third crack with a blue outline and closed cracks are shown with an X inside the circle as in Figure27.
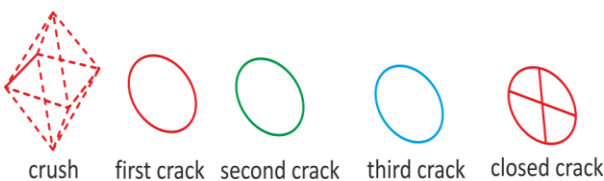
Fig. 27 Symbols Used by ANSYS to Represent Cracking and Crushing

The cracking pattern in the beam can be obtained using the crack/crushing plot option in ANSYS. Vector Mode plots must be turned on to view the cracking in the model. Figure28 and Figure29 show evolutions of crack patterns developed for each beam at the last converged loading step. The appearance of the cracks reflects the failure modes for the beams.
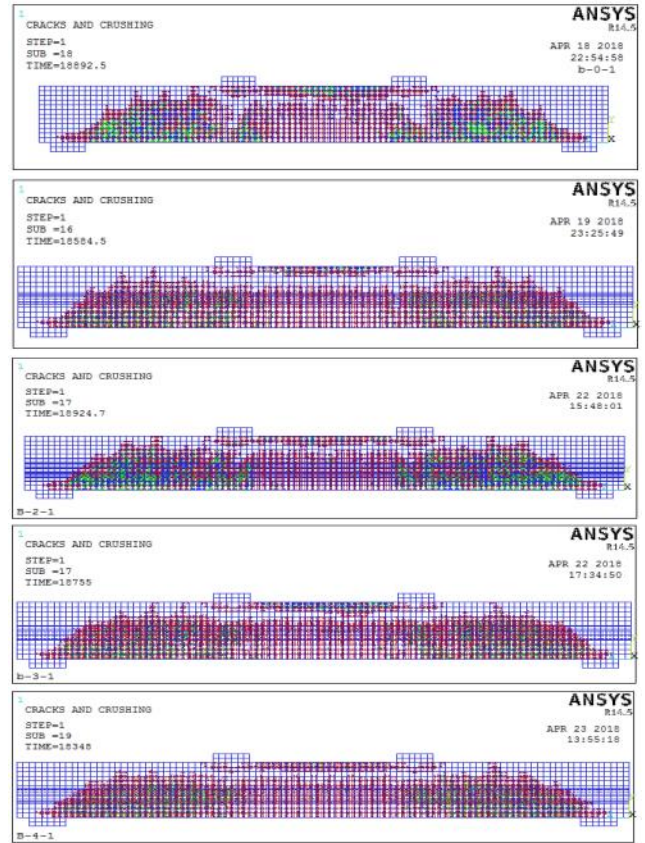
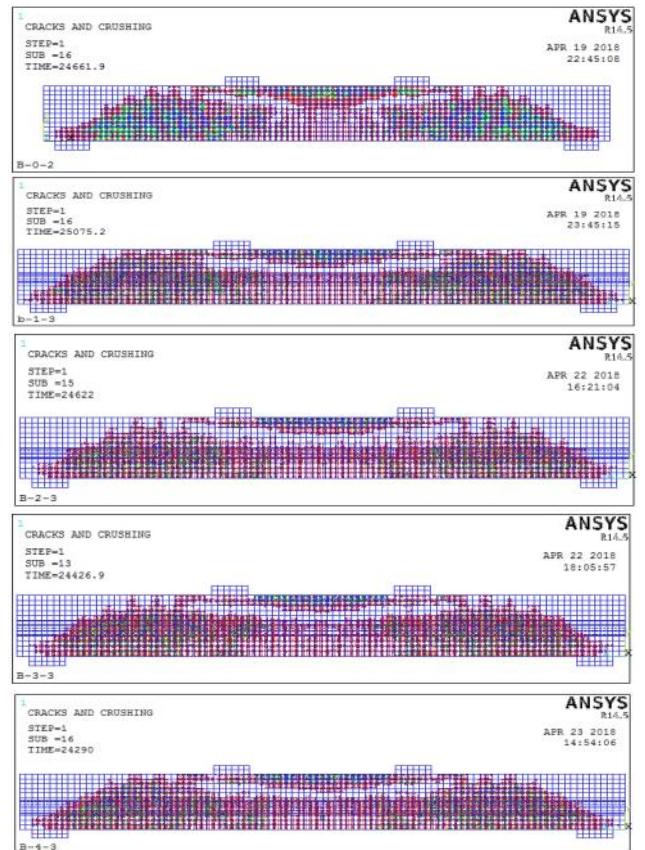**Fig. 28** Crack Pattern of Models with under Reinforced Section

Fig. 29 Crack Pattern of Models with over Reinforced Section

7.3 Stress Distribution

The finite element analysis provides stresses occurring at the integration points of solid elements. Maximum nodal stresses in concrete (plastic equivalent stress) (NLSEPL) and the nodal stresses in steel reinforcement (von-Mises stress) (SEQV) are obtained at the last converged load step and presented in form of contour lines as in Figure30 for beam model B-0-1 and Figure31 for beam model B-0-2.
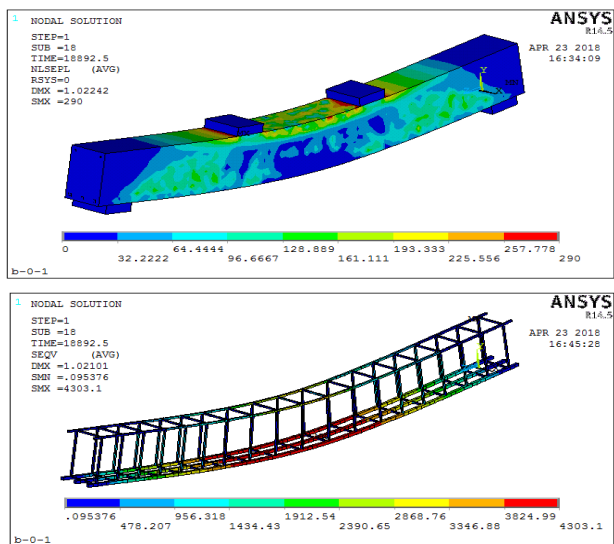

Fig.30 Stress in Concrete and Stress in Reinforcement for Model B-0-1
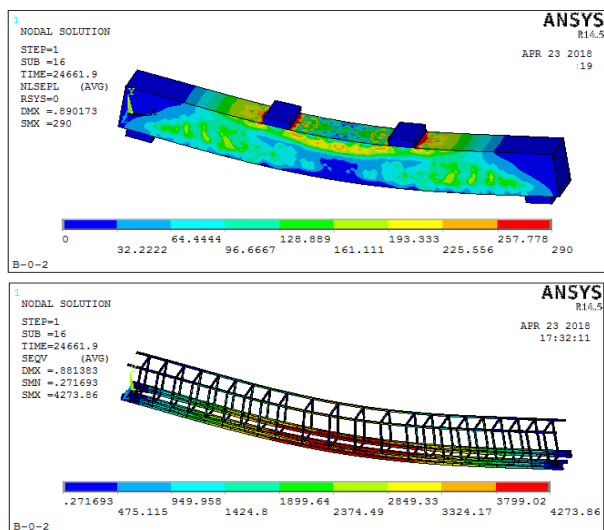

Fig.31 Stress in Concrete and Stress in Reinforcement for Model B-0-2

For the concrete once compressive stresses exceed the allowable compressive strength the failure will occur and this time recorded as failure time. For the steel when the equivalent stress exceeds the material yield stress, plastic deformation will occur. The maximum stress observed at bottom reinforcement in the mid-span of beam model.

Conclusions

1) The load carrying capacity of tested over reinforced beams (tensile reinforcement ratio 0.018) increased than tested under reinforced beams (low tensile reinforcement ratio 0.01) with percentage ranging between 19.70% and 39.25%
2) For over reinforced beams the stiffness and absorbed energy increased with percentage (15.89% to 29.32%) and (9.08% and 76.96%) respectively than tested under reinforced beams. But ductility index (μ_d) decreased with percentage (3.00% to 39.56%).
3) For beams with smaller PVC pipe diameter (50mm) at two investigated locations the load carrying capacity not affected where the load capacity increased with percentage ranging from (0.48% to 11.57%) than solid control beams for both under and over reinforced sections.
4) For beams with bigger PVC pipe diameter (75mm) their center location at 160mm the load carrying capacity not effected as the load capacity increased with percentage ranging from (7.69% and 9.64%) than solid control beam for both under and over reinforced sections.
5) But beams with PVC pipe diameter (75mm) their center location at 180mm the load carrying capacity of under reinforced section decreased with 10.85% than solid control beam while load carrying capacity of over reinforced section not affected and increased with 3.57% than solid control beam
6) For under and over reinforced beams that have the same diameter 50mm PVC pipes at two investigated locations (160mm and 180mm) the deflection decrease with percentage (9.99% to 33.96%) than solid control beam.
7) For under reinforced beams that have the same 75mm diameter PVC pipes at two investigated locations (160mm and 180mm) the deflection increased with percentage (14.65% and 23.19%) than solid control beam.
8) But for over reinforced beams that have the same 75mm diameter PVC pipes at two investigated locations (160mm and 180mm) the deflection decreased with percentage (22.72% and 27.61%) than solid control beam.
9) For both under and over reinforced beams the installation of PVC pipes decreases stiffness and absorbed energy with percentage ranging between (3.82% and 9.76%) and (8.78% and 36.18%) respectively than solid control beam.
10) Ductility index decreased for under reinforced beams that have 50mm diameter PVC pipes at two investigated locations (160mm and 180mm) with percentage (18.25% and 11.19%) than solid control beam
11) But over reinforced beams that have 75mm PVC pipes their ductility index increased with percentage ranging between (18.40% and 78.93%) than solid control beam.

12) In general the crack widths of beams with inserted PVC pipe were wider than solid beam and the cracks were distributed over the whole length of the reinforced beams but not reached to support as in solid beam also the failure modes were brittle shear failure.

13) The yield strain value of tension bar (0.002) was reached for all under reinforced beams with two inserted PVC pipe diameter at two investigated locations (160mm and 180mm) but ultimate strain value (0.003) reached only in case of beams with inserted PVC pipes their center at 160mm.

14) The yield strain value of stirrup (0.0012) was reached for under reinforced beams with inserted PVC pipes 75mm diameter but ultimate strain value (0.0016) reached in case of bigger PVC pipe diameter (75mm) and lower center position (180mm).

15) The yield strain value of tension bar (0.002) was reached for some over reinforced beams and ultimate strain value of all tension bar (0.003) not reached.

16) The yield strain value of stirrup (0.0012) was reached for over reinforced beams with smaller PVC pipe diameter (50mm) and wasn't reached for over reinforced beams with bigger PVC pipe diameter (75mm) (less concrete area to resist shear) .

17) It is visibly shown that the use of PVC pipe in tension zone had no significant influence if the diameter of the pipe is less than (0.25*b) at two studied location and if the diameter less than (0.375*b) for over reinforced section where (b) is the beam width.

18) The best location to install 50mm and 75mm PVC pipe in reinforced concrete beam is at 160mm (0.53*d) from the top of section away from the tension reinforcement to avoid brittle shear failure (d) is the beam depth.

19) Analytical results obtained from ANSYS program are in good assent with experimental results. As the maximum difference in estimating the failure load is (19.00%) also the load-deflection curves obtained from ANSYS are stiffer than that from the experimental data by value about (20.00%) this is due to ignoring concrete toughening mechanism.

References

ECP 203, (2017), Egyptian Code of Practice for Design and Construction of Concrete Structures, *Housing and Building National Research Center*, pp.4.3

Alnuaimi, Al-Jabri & Hago, (2008), Comparison between Solid and Hollow Reinforced Concrete Beams, *Materials and Structures*, Vol. 41, pp. 269-286

Jain Joy and Rajesh Rajeev, (2014), Effect of Reinforced Concrete Beam with Hollow Neutral Axis, *International Journal for Scientific Research & Development*, Vol. 2 Issue 10, ISSN: 2321-0613

Thaar Saud Salaman Al-Gasham, (2015), Reinforced Concrete Moderate Deep Beams with Embedded PVC Pipes, *Wasit Journal of Engineering Science* Vol. (3), No. (1), pp. 19-29

S.Manikandan, S.Dharmar and S.Robertravi, (2016), Experimental Study On Flexural Behavior Of Reinforced Concrete Hollow Core Sandwich Beams, *International Journal of Advance Research In Science And Engineering*, Vol 4, PP. 937-946,

Dhinesh.N.P and Satheesh.V.S, (2017), Flexural Behavior of Hollow Square Beam, *International Journal of Scientific Engineering and Applied Science*, Vol. 3, Issue-3, ISSN: 2395-3470

ANSYS, "ANSYS Help", Release 14.5, Copyright (2012)

Desayi, P. and Krishnan, (1964), Equation for the Stress-Strain Curve of Concrete, *Journal of the American Concrete Institute*, Vol. 61, pp. 345-350